



A novel Brayton cycle with the integration of liquid hydrogen cryogenic exergy utilization

Na Zhang^{a,*}, Noam Lior^b

^a*Institute of Engineering Thermophysics, Chinese Academy of Sciences, Beijing 100080, PR China*

^b*Department of Mechanical Engineering and Applied Mechanics, University of Pennsylvania, Philadelphia, PA 19104-6315, USA*

Received 12 May 2007; received in revised form 17 August 2007; accepted 17 August 2007

Available online 4 October 2007

Abstract

Stored or transported liquid hydrogen for use in power generation needs to be vaporized before combustion. Much energy was invested in the H₂ liquefaction process, and recovery of as much of this energy as possible in the re-evaporation process will contribute to both the overall energy budget of the hydrogen use process, and to environmental impact reduction. A new gas turbine cycle is proposed with liquefied hydrogen (LH₂) cryogenic exergy utilization. It is a semi-closed recuperative gas turbine cycle with nitrogen as the working fluid. By integration with the liquid H₂ evaporation process, the inlet temperature of the compressor is kept very low, and thus the required compression work could be reduced significantly. Internally fired combustion is employed to allow a very high turbine inlet temperature, and a higher average heat input temperature is achieved also by internal heat recuperation. As a result, the cycle has very attractive thermal performance with a predicted energy efficiency over 73%. The choice of nitrogen as the working fluid is to allow the use of air as the oxidant in the combustor. The oxygen in the air combines with the fuel H₂ to form water, which is easily separated from the N₂ by condensation, leaving the N₂ as the working fluid. The quantity of this working fluid in the system is maintained constant by continuously evacuating from the system the same amount that is introduced with the air. The cycle is environmentally friendly because no CO₂ and other pollutant are emitted. An exergy analysis is conducted to identify the exergy changes in the components and the potential for further system improvement. The biggest exergy loss is found occurring in the LH₂ evaporator due to the relatively high heat transfer temperature difference, dictated by the fixed temperatures of the LH₂ and of the ambient combustion air, which are far apart. The exergy efficiency is 45%. The system has a back-work ratio only $\frac{1}{4}$ of that in a Brayton cycle with ambient as the heat sink, and thus can produce 72.7% more work, with the LH₂ cryogenic exergy utilization efficiency of 50%. © 2007 International Association for Hydrogen Energy. Published by Elsevier Ltd. All rights reserved.

Keywords: Brayton cycle; Nitrogen; LH₂ cryogenic exergy; Hydrogen energy storage

1. Introduction

Hydrogen is a clean and versatile fuel and a good chemical energy carrier. It has a higher energy content per unit mass than any other fuel, but lower volumetric energy content due to the low density or high specific volume (12.3 m³/kg at 1 bar/298 K). For significant volume reduction it can be stored and transported much more conveniently in the compressed (0.069 m³/kg at 200 bar/298 K) or liquid state (0.014 m³/kg at 1 bar/20 K). Liquefaction reduces the volume 5-fold more than such compression, using cryogenic vessels which are rather common in the

industry and much lighter and safer than the ones needed for high pressure compressed hydrogen. This situation is quite similar to that of liquefied natural gas (LNG).

Hydrogen production and liquefaction, however, both require large amount of energy input and have impacts on the environment, leading to a reduction of energy utilization chain efficiency. Liquefaction, for example, needs ~ 36 MJ/kg H₂ at ambient pressure using current plants, and as low as 18 MJ/kg for proposed advanced systems. A considerable portion of this invested exergy is preserved in the LH₂, which, at 20 K, is at a temperature much lower than that of the ambient or of seawater. The liquid hydrogen needs to be re-evaporated to about the ambient temperature at the end of the storage chain. This offers the opportunity for using the ambient as a “free” heat

* Corresponding author. Tel.: +86 10 82543030; fax: +86 10 62575913.
 E-mail address: zhangna@mail.etp.ac.cn (N. Zhang).

Nomenclature

e	specific exergy, kJ/kg	η	energy efficiency
E	$\Delta e/\Delta h$, Eq. (4)	ε	exergy efficiency
H	enthalpy, kW	π	compressor pressure ratio
h	specific enthalpy, kJ/kg		
LHV	lower heating value, kJ/kg	<i>Subscripts</i>	
M	molar flow rate, kmol/s	a	energy acceptor
m	mass flow rate, kg/s	air	supplementary air
p	pressure, bar	b	boiling point
S	total entropy rate, kW/K	c	critical point
s	specific entropy, kJ/kg K	d	energy donor
T	temperature, K	dis	discharged N ₂ (stream 13)
t	temperature, °C	f	fuel
Q	heat duty, MW	L	liquid hydrogen
W	power output, MW	0	ambient state
ΔT_p	pinch point temperature difference, K	1...19	states on the cycle flow sheet

source, in a system where the liquefied hydrogen (LH₂) (or LNG) is the heat sink [1–13], for recovering power during the re-evaporation process needed for making the hydrogen (or LNG) usable for power production by combustion or fuel cells. From the energy perspective, this approach is clearly superior to conventional re-evaporation systems which just use the heat of seawater or ambient air, or even burn part of the gasified LH₂ or LNG without any concomitant power production.

Significant research was done on LNG cryogenic exergy recovery systems. Use of the cryogenic exergy of LNG for power generation includes methods which use the LNG as the working fluid in natural gas direct expansion cycles, or its coldness as the heat sink in closed-loop Rankine cycles [1–5], Brayton cycles [6–9], and combinations thereof [10,11]. Other methods use the LNG coldness to improve the performance of conventional thermal power cycles. For example, LNG vaporization can be integrated with compressor inlet air cooling in gas turbine power cycles [5,11,12], or in steam turbine condenser system (by cooling the recycled water [13]). Some pilot plants have been built in Japan from the 1970s, combining closed-loop Rankine cycles (with pure or multi-component organic working fluids) and direct expansion cycles [1].

Due to the increasing concern about greenhouse effects on climate change, the research and practice of CO₂ emission mitigation have become topics of great interest. The technologies available for CO₂ capture in power plants are mainly physical and chemical absorption, cryogenic fractionation, and membrane separation. The amount of energy needed for CO₂ capture could lead to the reduction of power generation efficiency by up to 10 percentage points [14,15].

Beside the efforts for reducing CO₂ emissions from existing power plants, concepts of power plants with zero CO₂ emission were proposed and studied. Deng et al. [9] proposed a nitrogen gas turbine cycle, in which the LNG cryogenic exergy was used not only for power generation, but also for CO₂ separation and recovery from the main combustion products. We have proposed and analyzed a novel CO₂ zero emission system integrated with an LNG evaporation process [16,17], which is

operated by a CO₂ quasi-combined two-stage turbine cycle with methane burning in an oxygen and recycled CO₂ mixture.

The physical cryogenic exergy of LH₂ can be used in the same way. With the primary combustion product being water, it produces no CO₂. However, since the LH₂ is at an even lower temperature, its direct use to cool the gas turbine inlet air or the steam turbine recycled cooling water, which may be done when operating in hot weather, would be associated with a large temperature difference in the heat exchangers, and thus causes high destruction of the LH₂ cryogenic exergy. To alleviate this problem, Bisio et al. [18] proposed a combined helium and combustion gas turbine plant. The bottoming helium Brayton cycle uses the topping gas turbine cycle exhaust as the heat source, and the LH₂ evaporation as the heat sink. It can fully exploit the temperature region with the bottoming cycle minimum temperature of 50 K, and an overall energy efficiency of 74% was predicted without hydrogen expansion (the evaporated hydrogen is at a pressure of 100 bar). This system does not, however, include CO₂ separation nor fully use the coldness exergy, letting the LH₂ exit the system still at the very low temperature of $-153\text{ }^\circ\text{C}$ ($\sim 120\text{ K}$), requiring heating by seawater to the ambient temperature.

In this paper, a novel system with simple configuration and the use of LH₂ cryogenic exergy is proposed and thermodynamically modeled. The main intention is to recover as much of the energy invested in the liquefaction process as possible, based on the fact that the stored H₂ needs to be evaporated for use anyway. The proposed system is a semi-closed recuperative gas turbine cycle with nitrogen as the working fluid. By integration with the liquid H₂ evaporation process, the inlet temperature of the compressor is kept very low, and thus the required compression work could be significantly reduced. In addition, a higher average heat input temperature is achieved by internal-fired combustion and exhaust heat recuperation. As a result, the cycle has a very attractive predicted thermal performance, with the energy efficiency near 73%. Our cycle has both high power generation efficiency and extremely low environmental impact.

2. The working fluid and cycle configuration

The lowness of the LH₂ storage temperature, of ~ 20 K 1 bar, makes it a very good power plant heat sink for increasing their efficiencies. If we use the same top temperature as those employed in current gas turbine cycles and simultaneously the minimal cycle temperature permitted by the LH₂ heat sink, the power cycle would operate with a temperature ratio of about 75, 15-fold higher than in conventional gas turbine cycles. A Brayton cycle is employed in this paper mainly for the following thermodynamic reasons: (a) the compression power can be reduced dramatically when the compressor inlet temperature is made low enough; (b) its performance is very attractive at these unusually high temperature ratios; (c) heat rejection at a varying temperature, in the form of sensible heat, matches well with the LH₂ supercritical evaporation process.

Internally fired combustion allows turbine inlet temperatures that are higher than externally fired, obviously because there is no need to transfer heat from the hot combustion products to the working fluid. To reduce the risk of unsafe mixing of oxygen with hydrogen in the cycle if leaks occur, the inert nitrogen gas is chosen as the working fluid instead of air: It allows the use of air as the oxidant in the combustor, is cheap, is essentially inert, and is safe [9]. In the evaporator *EVA*, the working fluid does contain oxygen, but its concentration is kept at a low level ($\sim 5\%$), and being at the ambient pressure level, it cannot be more dangerous than employing the *EVA* in ambient air as is commonly done.

Generally, the combustion-generated NO_x mainly has two sources: thermal NO_x, which is converted from nitrogen in the combustion air at high temperature, and fuel NO_x, which is converted from the nitrogen element contained in the fuel. With hydrogen as the fuel, there is no fuel NO_x. The generation rate of thermal NO_x highly depends on the combustion temperature and the oxygen concentration. Thermal NO_x is unlikely to be formed in noticeable quantities with low oxygen concentration and combustion temperature below 1300 °C; its impact has not been taken into consideration in this study.

In the nitrogen gas turbine cycle proposed by Deng et al. [9], the stoichiometric amount of air needed for the combustion, which is about $\frac{1}{3}$ of the compressor working fluid, is introduced at the compressor inlet, and mixed with the cold nitrogen. This increases the compressor inlet temperature and thus its power consumption (for the same inlet and outlet pressures). To better take advantage of the low temperature offered by LH₂, in the system proposed in this paper (Fig. 1), the supplementary air is mixed with the nitrogen before being cooled by the LH₂. The introduced air should be dehumidified to avoid frost formation in the LNG evaporator *EVA*. This could be accomplished in a number of ways, and an effective solution that starts by first cooling the incoming air (stream 1) just sufficiently to condense out the water, followed by desiccant dehumidification to remove the remaining water vapor, was described in [12]. The cooling could easily be accomplished in our cycle by using one of the cold streams between 1 and 5 °C, and desiccant dehumidification of air is standard commercial practice. Since there are different methods for avoiding frosting, and since they con-

sume very little power, they were not considered in our analysis quantitatively.

Since air and a small fraction of the vaporized LH₂ for the combustion are introduced at the stoichiometric ratio, alongside with the recirculated N₂, the combustion products are merely water and N₂. The cycle heat rejection process has a good temperature match with the LH₂ supercritical evaporation process. Water is condensed out and the surplus N₂ is extracted from the system in the cycle heat rejection process. The cycle is environmentally friendly because no CO₂ and other pollutant are emitted. Use of any other working fluid, except air (that has an O₂ concentration higher than the auto-oxidation limit for H₂), would require continuous separation of that working fluid from the N₂ entering with the air, or an air separation unit that allows the use of pure oxygen in the combustor. Such a unit typically consumes about 800–900 kJ power for producing 1 kg O₂, and thus would have imposed a large penalty on the overall system thermal efficiency.

To prevent steel embrittlement due to nitriding at these high operating temperatures [7,9], additional oxygen ($\sim 0.5\%$ by volume) is maintained in the combustion products. Consequently, a small fraction of oxygen is expelled along with the discharge of the extra nitrogen. By properly controlling the complementary air amount at the inlet of the mixer *MIX*, the oxygen mass balance is maintained inside the system. As compared with other inert gases, such as helium, nitrogen offers the additional advantage of real gas behavior in the lower temperature range, whereby the required compression power is further reduced [7].

Some related thermal properties of N₂ and H₂ are shown in Table 1.

The base-case cycle layout and the corresponding *t*–*S* diagram are shown in Figs. 1 and 2, respectively.

The Brayton cycle can be identified as 1 and 2 → 3 → 4 → 5 → 6 → 7 → 8 → 9 → 10 → 11 and 12. Supplementary air (1) and N₂ (2) mix and reject heat in the LH₂ evaporator *EVA*, being cooled down to the cycle lowest temperature level. This cooling reduces the compression work. The mixture (4) is compressed, and then preheated in *REP* by the turbine exhaust gas heat before entrance to the combustor *COM*.

A small fraction of vaporized hydrogen is introduced in the combustor as the fuel. Assuming stoichiometric combustion, the exhaust gas of the Brayton cycle contains the combustion products H₂O through the path 7 → 8 → 9 → 10. After releasing heat in *REP*, the exhaust gas is cooled further, by heating the H₂ in *HEX*, which brings its temperature to 5 °C, and most of the vapor is separated from the N₂ by condensation and withdrawal in the separator *SEP* to reduce the dehumidifier load. The minute amount of vapor in the working fluid after a flash separation can be completely removed by adsorption.

The LH₂ evaporation process is 14 → 15 → 16 → 17 → 18 and 19. LH₂ unloaded from its storage (14) is first pumped by pump *P* to its evaporation pressure (15), and then heated in the evaporation system (*EVA* (16) and *HEX* (17)) to about ambient temperature.

The proposed system produces power and evaporates the LH₂ for further use, while preventing $\sim 50\%$ of the LH₂ cold exergy

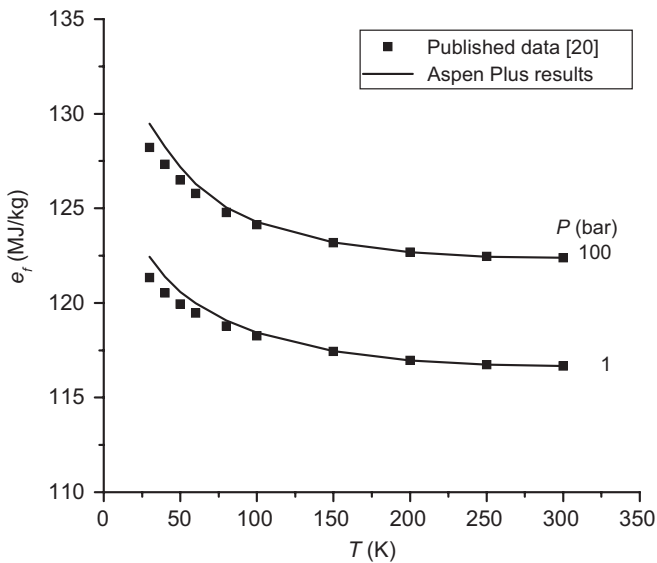


Fig. 3. H₂ property calculation validation.

in the temperature region of 30–300 K, was found. The exergy values in Fig. 3 were calculated by Aspen Plus, calibrated with the method in [21], which include both chemical and physical exergy.

We found that, however, the property calculation has bigger error in the temperature region < 30 K. For the LH₂ evaporation process below 30 K, the entropy curve exhibits anomalous behavior. To eliminate this error, we assumed that the LH₂ is unloaded at a temperature of 30 K with the corresponding saturation pressure of 8.12 bar. This assumption slightly affects the LH₂ pump work, but has negligible effect on the global system performance. To simplify computation, it was assumed that the system operates at a steady-state, the combustion is stoichiometric with H₂O the primary combustion product, no turbine blade cooling, and the stoichiometric amount of the water evacuated from the cycle does not contain dissolved working fluid.

The most important assumptions for the calculations in this paper are summarized in Table 2.

The cycle minimal temperature is chosen as –190 °C to avoid working fluid condensation, since the saturation temperature of N₂ under ambient pressure (1 bar) is –196 °C (Table 1).

The energy efficiency is calculated as the ratio between overall power output and heat input of the Brayton cycle [11]:

$$\eta = W / (m_f \cdot LHV), \quad (1)$$

where W is the overall power output from the turbines, reduced by the power input to the compressor (C) and pump (P), and the mechanical and generator losses, m_f is the fuel mass flow rate. This cycle employs both fuel and LH₂ coldness (via its evaporation) as its input resources, but in the definition of η we have used only the fuel energy, because the LH₂ coldness is free, and its reduction through the evaporation is actually needed by the user. Both input resources are, however, used in defining ε , the exergy efficiency, which is the more appropriate criterion for performance evaluation than the fuel energy alone.

Table 2

Main assumptions for the calculation

Main assumptions for the calculation	
Cycle parameters	
Ambient temperature (°C)	25
Ambient pressure (bar)	1.013
Minimum temperature t_4 (°C)	–190
H ₂ LHV (kJ/kg)	119,974
Turbine T	
Inlet temperature t_7 (°C)	1200
Isentropic efficiency (%)	90
Compressor C	
Pressure ratio π	15
Isentropic efficiency (%)	87
Combustor COM	
Efficiency (%)	100
Pressure loss (%)	3
Separator SEP	
Working temperature (°C)	5
Recuperator REP	
Pressure loss (%)	3
LH ₂ vaporization system (EVA and HEX)	
LH ₂ pump efficiency (%)	75
Pressure loss (%)	3
Evaporation pressure (bar)	100
Mech. and generator	
Efficiency (%)	96

It is defined here as the ratio between the net obtained and total consumed exergy:

$$\varepsilon = W / (m_f \cdot e_f + m_L \cdot e_L), \quad (2)$$

where m_L is the treated LH₂ mass flow rate and e_L the exergy difference between the initial and the final states of the LH₂ evaporation process:

$$e_L = (h_{15} - h_{17}) - T_0(s_{15} - s_{17}). \quad (3)$$

For a given mass flow rate of the cycle working medium, the mass flow rates of needed fuel, of water recovered, and of the regasified LH₂ can all be determined.

With 100 kg/s mass flow rate of N₂ at the mixer MIX inlet (stream 2 in Fig. 1) taken as a reference, Table 3 summarizes the main parameters, including temperature, pressure, flow rate, and composition, of each stream for the supercritical pressure (100 bar) hydrogen delivery. The mass flow rate of evaporated LH₂ is found to be 12.7 kg/s, of which about 7.7% (0.98 kg/s) are sent to the combustor as fuel for the cycle; and the water recovered and supplementary air amounts are found to be 8.8 and 34.1 kg/s, respectively.

The computed performance of the cycle is summarized in Table 4. The net power produced is found to be 86 MW, resulting in a thermal efficiency (η) of 73% and exergy efficiency (ε) of 45%. The difference between the efficiencies is due to their definition (Eqs. (1) and (2)), where η does not take into account the LH₂ coldness energy, while ε does.

The t – Q (Q is the heat duty of a heat exchanger) diagrams for the heat exchangers in the recuperation system (REP and HEX) and the LH₂ evaporation system (HEX and EVA) are shown in Figs. 3 and 4, respectively. The heat load is not distributed evenly among the different heat exchangers. More than 80% of

Table 3
The main stream parameters of CO₂ cycle^a

No.	<i>t</i> (°C)	<i>p</i> (bar)	<i>m</i> (kg/s)	Molar composition			
				O ₂	N ₂	H ₂ O	H ₂
1	25	1.013	34.14	0.21	0.79	0	0
2	5	1.013	100	0.005	0.995	0	0
3	10	1.013	134.14	0.056	0.944	0	0
4	−190	1	134.14	0.056	0.944	0	0
5	−74.2	15.9	134.14	0.056	0.944	0	0
6	542.9	15.45	134.14	0.056	0.944	0	0
7	1200	15	135.12	0.005	0.898	0.098	0
8	572.9	1.07	135.12	0.005	0.898	0.098	0
9	42.9	1.04	135.12	0.005	0.898	0.098	0
11	5	1.013	8.305	0	0	1	0
13	5	1.013	26.34	0.005	0.995	0	0
14	−243.3	8.12	12.74	0	0	0	1
15	−231.6	103	12.74	0	0	0	1
16	−97.2	101	12.74	0	0	0	1
17	15	100	12.74	0	0	0	1
18	15	15.45	0.983	0	0	0	1

^aMIX inlet N₂ (stream 2) mass flow rate of 100 kg/s assumed as references.

Table 4
Performance summary

	Base-case
Turbine work (MW)	107.9
Compressor work (MW)	15.32
LH ₂ pump work (MW)	2.96
Mechanic and generator loss (MW)	3.55
Net power output <i>W</i> (MW)	86.07
LH ₂ mass flow rate (kg/s)	12.74
Fuel ratio (%)	7.7
Fuel energy input <i>m_f · LHV</i> (MW)	117.93
LH ₂ exergy input <i>m_L · e_L</i> (MW)	72.74
Energy efficiency <i>η</i> (%)	73.0
Exergy efficiency <i>ε</i> (%)	45.1

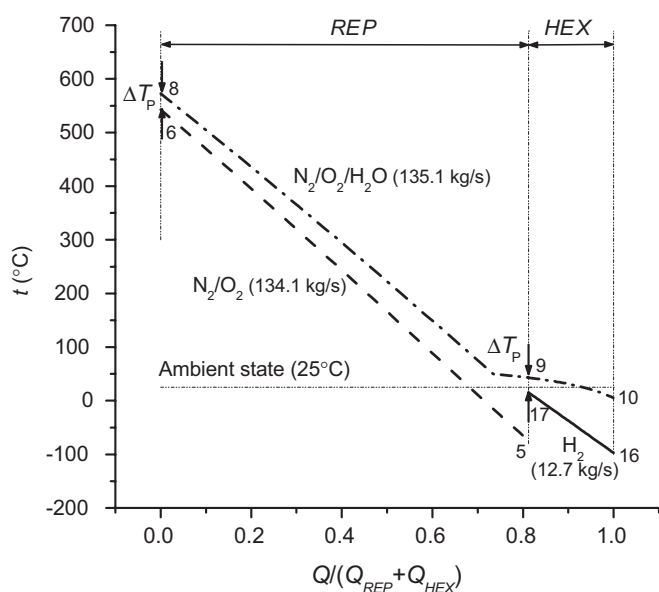


Fig. 4. *t*–*Q* diagram in the recuperation process.

the turbine exhaust heat is recovered in *REP*, to heat the working fluid before it enters the combustor. The turbine exhaust temperature gradually decreases at it passes through *REP*, at a lower rate, when the contained H₂O vapor starts condensing. The 94.5% of the steam is condensed at the *SEP* entrance. By simple gas–liquid phase separation, the working fluid vapor content is only 0.4% by mass. Complete removal of this vapor is assumed in the dehumidifier.

The minimal temperature differences are present at the hot end of *REP* and *HEX*. The minimal temperature difference, ΔT_p , is 30 K in the recuperator. The working fluid temperature is 43 °C at the inlet of *HEX*; it heats the H₂ to a temperature of 15 °C.

Due to the integration with the LH₂ evaporation process, the required back-work ratio (the compressor work consumption divided by the turbine work output) is 0.14, which is $\frac{1}{4}$ of that with ambient as the cycle heat sink.

Reducing the pinch point temperatures will increase the thermal performance, but larger heat transfer surface area and more equipment investment will be required.

In the LH₂ evaporation system (*HEX* and *EVA*), about 58% of the needed heat is added in the evaporator *EVA*. The average heat transfer temperature difference is about 78 °C, which is relatively high and therefore would cause big exergy loss in the evaporation process.

4. Exergy analysis

Exergy analysis is conducted to locate the major exergy losses in the system, so that pertinent guidance could be provided for system performance improvement. The results are reported in Table 5.

It can be seen that the total exergy input to the system is about 190.7 MW, from which the LH₂ cold exergy contribution is about 38%. Besides the net power output, the system exergy

Table 5
System exergy breakdown

	Exergy (MW)	Exergy (%)
Exergy input		
Fuel	118.0	61.86
LH ₂	72.74	38.14
Exergy output		
W	86.07	45.12
N ₂	0.57	0.29
Component exergy change		
EVA	42.98	22.53
COM	30.0	15.73
REP	9.38	4.92
HEX	6.96	3.65
T	4.42	2.32
C	3.09	1.62
P	2.96	1.55
MIX	0.777	0.41
SEP	0.048	0.03
Mech. and gen. loss	3.55	1.86
Summation	104.18	54.61

output also includes the exergy in the emerging streams of nitrogen and hydrogen. The produced N₂ stream (13) accounts for a minute value of 0.3% of the total exergy input. Although the H₂, one of the system output streams, is delivered at a pressure of 100 bar, its pressure-associated physical exergy is not included among the exergy outputs in Table 5 because the LH₂ exergy input is calculated based on the evaporator EVA entry state of the same pressure, 100 bar/−232 °C.

The total exergy drop in the components, defined as the change in exergy between the entry state and the exhaust state of each process, is 52.75%. This exergy change in each process can be regarded as the sum of two terms: exergy used and exergy loss. The exergy used is defined by the change in exergy when the process is executed reversibly, which is necessary to accomplish the objective of the process by using that component. The exergy loss is determined by subtracting the exergy used from the actual exergy change, and is attributable to the irreversibility of the process, which can be reduced as the process approaches reversibility.

The biggest exergy change is in the LH₂ evaporator (EVA), where LH₂ is heated by the mixture of N₂ and a small fraction of O₂ (~5% by volume). As mentioned before, restricted by the N₂ boiling point temperature of about −196 °C, the minimum cycle temperature is chosen to be −190 °C (83.15 K) to avoid the working fluid condensation. This leads to a relatively big average temperature difference in the evaporation process and correspondingly higher exergy destruction.

One way to reduce the exergy destruction due to the large temperature differences in EVA is to try and exploit its available very low temperature of 20 K (−253 °C). This could be done by switching the working fluid from nitrogen to helium, due to its much lower critical point temperature (4.125 K) [18]. Choosing helium would, however, require either a closed gas cycle with external heating, and the cycle top temperature would be limited by the current material technology; or the employment of an air separation unit to produce oxygen as the oxidant in the

combustor, so that the combustion product is only helium and water, and then water is separated and helium recirculated. The first was already investigated by Bisio et al. [18]; it is worthy to do a comparison with the latter. Another option for reducing this large exergy change is to reduce the temperature of the air+nitrogen mixture fed to EVA (stream 3 in Fig. 1). This could be done by precooling stream 3 by the compressor outlet stream 5, upstream of REP, using an additional heat exchanger. This potential improvement was not analyzed here, and both the mentioned improvement possibilities demonstrate the value of the design guidance that exergy analysis offers.

As expected, a large exergy change also occurs in the combustion process because the fuel chemical exergy is destroyed and converted into the thermal exergy. If the fuel chemical exergy could also be used in a cascade, the combustion-generated exergy change would be decreased. One example of such an approach is a power cycle that combines a fuel cell with a gas/steam turbine [22]. The fuel chemical exergy is first converted into electricity directly in the fuel cell, and then the lower affinity exhaust energy is used efficiently in a thermal power plant.

The heat transfer process in the recuperator REP accounts for 4.9% of the total system exergy input, which can be reduced if smaller heat transfer temperature difference was employed, with the associated cost of bigger heat transfer area surface.

The exergy changes in these three heat exchangers (EVA, COM, REP) are over 31% of the total components' exergy input.

To analyze these heat transfer processes with an aim of reducing exergy destruction, it is effective to use the ratio of the exergy and energy change, E , defined as

$$E = \Delta e / \Delta h, \quad (4)$$

which that shows the effect of enthalpy changes on the concomitant exergy ones.

Recalling that the exergy change of a stream with temperature T , enthalpy h , and entropy s to an associated environment (dead) state T_0, h_0, s_0 , is

$$\Delta e = (h - h_0) - T_0 \cdot (s - s_0) \quad (5)$$

and thus E becomes

$$E = \Delta e / (h - h_0) = 1 - T_0 \cdot \frac{s - s_0}{h - h_0}. \quad (6)$$

Defining the entropic average temperature as $T = (h - h_0) / (s - s_0)$ gives

$$E = 1 - (T_0 / T), \quad (7)$$

for $T > T_0$.

In this case, E is equivalent to the power produced in a Carnot cycle working between T and T_0 with unit heat input. It is always smaller than 1, and is defined as the availability factor or the energy quality [23]. Based on this concept, Ishida et al. proposed the graphical exergy analysis method—exergy utilization diagram (EUD) [23,24]. In each energy-transformation system, the EUD method identifies an energy donor and an

energy acceptor. Energy is released by the former and is accepted by the latter as ΔH , and the energy qualities of the donor E_d and acceptor E_a are paired. By plotting E_d and E_a vs the transformed energy ΔH , we obtain the exergy loss represented as the area in between. Compared with the $T-Q$ diagram, which interprets the process from the energy point of view, the EUD does it from both the energy and exergy ones: ΔH (or Q) on the abscissa represents the transferred energy quantity related to the first law of thermodynamics; while E on the ordinates denotes the corresponding energy quality (exergy) and is related to the second law of thermodynamic. In addition, $\Delta E = E_d - E_a$ is an indicative parameter and represents the driving force to make the process proceed. The smaller it is, the smaller the irreversibility of the process will be. Corresponding to the minimum temperature difference ΔT_P in the $T-Q$ diagram, where a smallest ΔE is identified, a pinch is found at that location. This method obviously provides more information than just the exergy difference between the entry and exit states.

Similarly, the minimal work needed to bring a stream from the environment to a state with a temperature $T (T < T_0)$ is equal to $-E = (T_0/T - 1)Q$, which is equivalent to the power needed to produce a unit of refrigeration by a Carnot refrigeration cycle working between T_0 and T . Since we did not find a prior EUD treatment of processes that takes place at below-ambient temperatures, the following elaboration expands the use of the EUD method to this particular case. This minimal work increases very strongly as the temperature drops in the cryogenic region. Eq. (7) can therefore also be used for the calculation of E for $T < T_0$, producing a negative value because power input is needed for producing the refrigeration. In this case the energy quality indicator is $|E|$ instead of E . If the energy donor and acceptor thus both have negative values of E , then the energy donor is the exergy acceptor, and the energy acceptor is the exergy donor, which means that the exergy flows in a direction opposite to that of the energy flow.

To summarize, for $E_d \times E_a > 0$, which means that the temperatures of both the energy donor and the energy acceptor are $> T_0$, or both are $< T_0$, exergy flows from the side with higher $|E|$ to that of the lower $|E|$. A very special case is that of $E_d \times E_a < 0$, which is a process in which the energy donor is above the ambient temperature and the energy acceptor is below the ambient temperature. In this case they both are the exergy donor, and the environment is the exergy acceptor. The area between the E_d and E_a curves still represents the process exergy change. By using $|E|$ as the energy quality (exergy) indicator, we extend the EUD method into the region below the ambient temperature.

For comparison with the energy analysis result ($t-Q$ diagrams in Figs. 4 and 5), we can draw $E-Q$ diagrams for the heat exchangers (REP, EVA, and HEX) as shown in Fig. 6. It should be noted that these Figs. 4–6 describe the same heat transfer process in REP, EVA, and HEX, $t-Q$ diagram from the energy viewpoint, and the $E-Q$ diagrams describe them from both the energy and exergy one.

In Fig. 6, obviously REP has the biggest heat quantity transferred (88.9 MW), but the exergy change is not very high as represented by the corresponding shaded area. The energy donor

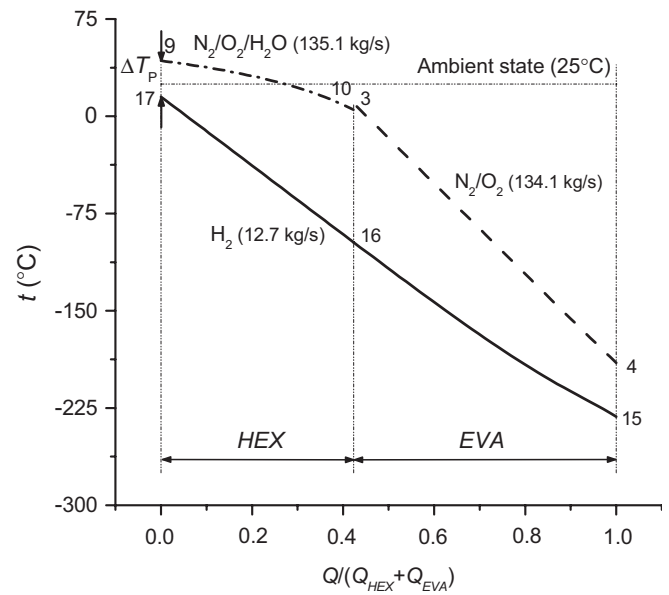


Fig. 5. $t-Q$ diagram in the LH₂ evaporation process.

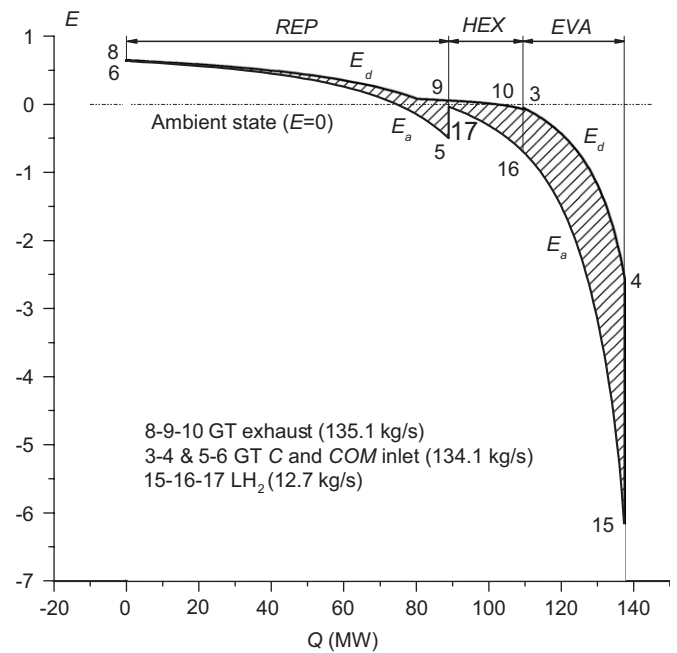


Fig. 6. $E-Q$ diagram in the heat exchangers.

8–9 is the hot turbine exhaust gas with an average $E = 0.408$, and the energy acceptor is the pressurized compressor working fluid with an average $E = 0.303$. ΔE is only 0.105, leading to a smaller energy change of 9.4 MW of the process.

On the contrary, the energy quantity processed in EVA is much lower (28 MW), but the corresponding exergy change is much higher (43 MW). In EVA, both the exergy donor and the acceptor temperatures are under the ambient, with negative E . LH₂ (15–16) receives heat (energy) from the working fluid (3–4), but the exergy flows in the opposite direction, from LH₂,

with $|E| = 2.38$ to the working fluid with a lower $|E|$ ($=0.85$). The relatively bigger $\Delta E = 1.53$ results in the higher exergy change.

In *HEX*, the heat transfer is from the turbine exhaust (9–10) to the cold evaporated H_2 (16–17) with the average $\Delta E = 0.33$. The exergy exchange is more complex; it can be divided into two sections: in the lower temperature section with both E_d and $E_a < 0$ ($E_d \times E_a > 0$), the exergy is transferred from H_2 to the turbine exhaust, while in the higher temperature section, $E_d > 0$ and $E_a < 0$ ($E_d \times E_a < 0$), both H_2 and the turbine exhaust lose exergy to the environment. This happens in *REP* too where E_d curve also crosses the $E = 0$ line.

Also in Fig. 6, two smallest values of ΔE are found at the hot end of *REP* and *HEX*, which are 0.013 and 0.091, respectively, corresponding to the pinch point positions in the $t-Q$ diagram in Fig. 4. In *EVA*, ΔE increases fast as the temperature drops in the low temperature region. It becomes 3.6 at the cold end, indicating a larger exergy loss there. As mentioned before, this is caused by the relatively larger temperature difference between the working fluid and the LH_2 .

5. Performance and discussion

The Brayton cycle turbine inlet temperature t_7 and the compressor pressure ratio are the key system parameters. Their influences on the cycle performance are investigated, and the results are shown in the Figs. 7–9.

From Fig. 7, as the turbine inlet temperature or pressure ratio increases, the fuel demand increases too. Proportional quantities of air are added as the oxidant. To maintain the balance of the working fluid, the nitrogen contained in the supplementary

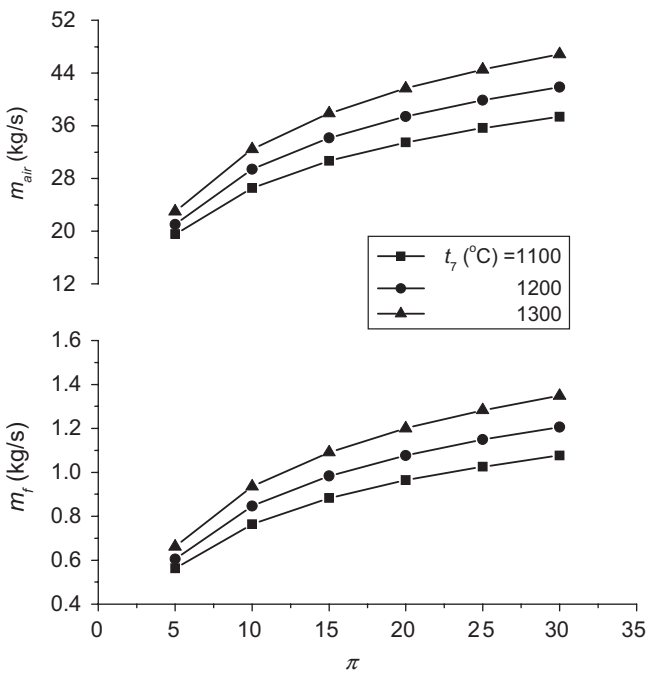


Fig. 7. The effect of pressure ratio on the supplementary air and fuel mass flow rates.

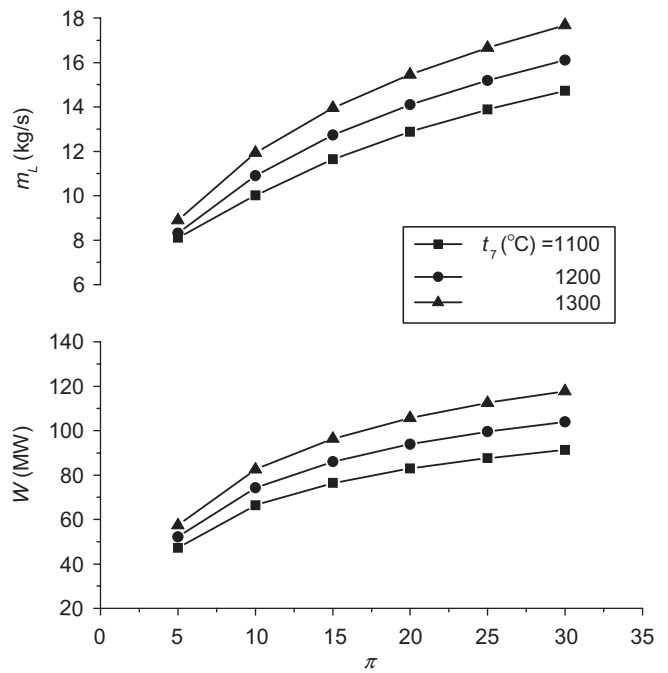


Fig. 8. The effect of pressure ratio on the power output and the processed LH_2 mass flow rate.

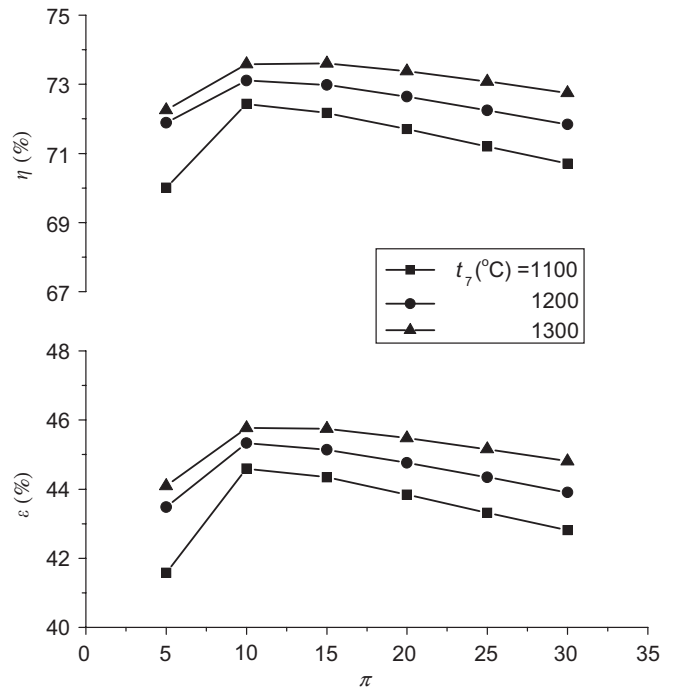


Fig. 9. The effect of pressure ratio on the efficiencies.

air needs to be continuously evacuated from the working fluid (stream 13 in Fig. 1). As mentioned before, additional oxygen (0.5% by volume) should be maintained in the hot path of the system to prevent the material nitrification. Assuming that the air molar composition is $O_2 : N_2 = 0.21 : 0.79$, the introduced

air amount and the fueled H_2 in mol follow the equation:

$$M_{\text{air}} = 0.5M_f / (0.21 - 0.005 \times 0.79) = 2.4266M_f. \quad (8)$$

Correspondingly, a proportional amount of N_2 needs to be evacuated after the water is removed and collected in the separator SEP. In fact the vented gas is also a mixture of N_2 and O_2 (99.5% N_2 and 0.5% O_2 by volume); so the discharged mol amount is

$$M_{\text{dis}} = 0.79 \cdot (1 + 0.005)M_{\text{air}} = 0.79395M_{\text{air}} = 1.9266M_f. \quad (9)$$

As shown in Fig. 8, when the turbine inlet temperature and cycle pressure ratio increase, the working fluid mass flow rate increases too because of the above-described introduction of more air and fuel introduction, which leads to an additional increase in the cycle power output. At the same time, the working fluid temperature at the inlet of *HEX* increases too; therefore, more heat is available for the LH_2 evaporation and more LH_2 could be processed as a result.

The effect of the pressure ratio on the efficiencies is shown in Fig. 9. When the turbine inlet temperature t_7 increases, both efficiencies increase, but the increase is less than 1 percentage point for 100°C increase in t_7 . The efficiency increase stops at a pressure ratio of about 10, which maximizes the efficiencies. The existence of maximal efficiency and power output is typical to Brayton cycles, and the corresponding pressure ratio values highly depend on the cycle temperature ratio. The pressure ratio that produces the highest cycle efficiency increases with the temperature ratio, but with turbine exhaust heat recuperation, as used in this cycle, that pressure ratio is much lower, but recuperation has almost no impact on the optimal pressure ratio for power output. The pressure ratio that maximizes the power output is much higher than 30 (the upper limit of this calculation) because of the extremely high temperature ratio of the cycle. Also with recuperation, the pressure ratio for maximal cycle efficiency is a very weak function of the temperature ratio.

A conventional N_2 Brayton cycle with the same thermodynamic conditions (Table 2), but with the environment as the heat sink, can produce 49.82 MW power. The additional power produced by the system with LH_2 as the heat sink is 36.25 MW (2.85 MJ/kg LH_2), with this 72.7% higher power production being the contribution of the LH_2 cryogenic exergy. This can be seen as a recovering part of the energy spent for hydrogen liquefaction: 7.9% of the invested energy for the current liquefaction technology and 15.8% for the advanced liquefaction technology. The exergy input from LH_2 evaporation is 72.7 MW; therefore, an estimated 50% of the LH_2 cryogenic exergy is recovered in this cycle.

6. Conclusions

A novel power cycle with integration of LH_2 cryogenic exergy utilization is proposed and thermodynamically modeled. The proposed system is intended to be used at the end of the LH_2 storage or transportation chain, to recover in the re-evaporation process some of the energy originally invested for the H_2 liquefaction.

The system produces power, evaporated LH_2 , and recovered water from the combustion. Good thermodynamic performance can be obtained using conventional technologies, with the energy and exergy efficiencies reaching 73% and 45%, respectively. This excellent performance is attributed to the following characteristics:

- (1) very low compressor inlet temperature due to the direct heat exchange with LH_2 ;
- (2) high turbine inlet temperature with internal-fired combustion;
- (3) high average heat addition temperature with turbine exhaust heat recuperation;
- (4) no flue gas sensible heat loss to the environment;
- (5) full exploitation of the LH_2 evaporation process.

Beside the attractive thermodynamic performance, the system has some other merits including

- (6) negligible release of pollutants (neither in energy nor in species) to the environment;
- (7) high reliability and low cost in operation due to the simple design of the system;
- (8) no need for cooling water; on the contrary, the combustion-generated water can be recovered for use;
- (9) the discharged nitrogen is at high purity, and can be used for some other chemical or industrial purposes.

The influences of some key parameters on the cycle performance, including the Brayton cycle turbine inlet temperature ratio and pressure ratio, were studied. It was found that there is a pressure ratio, of about 10, which maximizes the efficiencies, and that the pressure ratio that maximizes the specific power output is much higher.

The exergy analysis produced the exergy change distribution in the components, and suggests the potential for further improvement. The authors defined the energy quality indicator in the temperature region below the ambient temperature, and expanded the application of the EUD method into that temperature region. It was found that the biggest exergy change occurs in the LH_2 evaporator due to the relatively higher heat transfer temperature difference. This is to some extent dictated by the fact that the cycle minimal temperature is restricted by the working fluid boiling point temperature. To further decrease the cycle minimum temperature for fully exploiting the lowest temperatures offered by the LH_2 , helium, which has a much lower boiling temperature than nitrogen, could be a proper working fluid. The disadvantage of using helium is, however, that either an air separation unit or an externally fired combustor would need to be employed to avoid the blending of the He with N_2 entering with the air, which may impose a penalty on the system thermal performance and make the system more complex, but a detailed investigation of this approach is warranted.

In comparison, a conventional Brayton cycle with the same working fluid and thermal conditions, but using the environment as the heat sink, would produce 36.2 MW, less power (a reduction of 42.1%). This amount of power output can be

regarded as the contribution of the LH₂ cryogenic exergy. With the system proposed and analyzed, nearly 50% of the LH₂ cryogenic exergy is converted into power.

Acknowledgment

The first author gratefully acknowledges the support of the Chinese National Key Fundamental Research Project (No. 50520140517).

References

- [1] Karashima N, Akutsu T. Development of LNG cryogenic power generation plant. in: Proceedings of 17th IECEC 1982; p. 399–404.
- [2] Angelino G. The use of liquid natural gas as heat sink for power cycles. ASME J Eng Power 1978;100:169–77.
- [3] Kim CW, Chang SD, Ro ST. Analysis of the power cycle utilizing the cold energy of LNG. Int J Energy Res 1995;19:741–9.
- [4] Najjar YSH, Zaamout MS. Cryogenic power conversion with regasification of LNG in a gas turbine plant. Energy Convers Manage 1993;34:273–80.
- [5] Wong W. LNG power recovery. Proc Inst Mech Eng A J Power Energy 1994;208:1–12.
- [6] Zhang N, Cai R. Principal power generation schemes with LNG cryogenic exergy, in: Proceedings of ECOS'02, Berlin, Germany; 2002. p. 334–41.
- [7] Krey G. Utilization of the cold by LNG vaporization with closed-cycle gas turbine. ASME J Eng Power 1980;102:225–30.
- [8] Agazzani A, Massardo AF. An assessment of the performance of closed cycles with and without heat rejection at cryogenic temperatures. ASME J Eng Gas Turbine Power 1999;121:458–65.
- [9] Deng S, Jin H, Cai R, Lin R. Novel cogeneration power system with liquefied natural gas (LNG) cryogenic exergy utilization. Energy 2004;29:497–512.
- [10] Chiesa P. LNG receiving terminal associated with gas cycle power plants. ASME Paper 97-GT-441. New York: ASME; 1997.
- [11] Kim TS, Ro ST. Power augmentation of combined cycle power plants using cold energy of liquefied natural gas. Energy 2000;25:841–56.
- [12] Hisazumi Y, Yamashita S, Fukuyoshi Y, Nakamura K. The development of the hybrid vaporization and power generation system for the gas turbine using LNG cold. In: Proceedings of PWR 2005, Paper 2005-50363, ASME power conference, Chicago, Illinois USA; April 5–7, 2005.
- [13] Desideri U, Belli C. Assessment of LNG regasification systems with cogeneration. In: Proceedings of TurboExpo 2000, Munich, Germany Paper 2000-GT-0165. New York: ASME; 2000.
- [14] Riemer P. Greenhouse gas mitigation technologies, an overview of the CO₂ capture, storage and future activities of the IEA greenhouse gas R&D program. Energy Convers Manage 1996;37:665–70.
- [15] Haugen HA, Eide LI. CO₂ capture and disposal: the realism of large scale scenarios. Energy Convers Manage 1996;37:1061–6.
- [16] Zhang N, Lior N. A novel near-zero CO₂ emission thermal cycle with LNG cryogenic exergy utilization. Energy 2006;31:1666–79.
- [17] Zhang N, Lior N. Proposal and analysis of a novel zero CO₂ emission cycle with LNG cryogenic exergy utilization. ASME J Eng Gas Turbine Power 2006;128:81–91.
- [18] Bisio G, Massardo A, Agazzani A. Combined helium and combustion gas turbine plant exploiting liquid hydrogen (LH₂) physical exergy. ASME Paper 95-GT-298. New York: ASME; 1995.
- [19] Aspen Physical Property System. Physical property methods and models 11.1. Cambridge, MA: Aspen Technology, Inc.; 2001.
- [20] Perry RH, Green DW. Perry's chemical engineers handbook, 6th ed. New York: McGraw-Hill; 1984.
- [21] Zheng DX, Wu XH, Zheng DS. Fundamental of thermodynamic consistency of exergy functions. J Chem Ind Eng (China) 2002;53: 673–9.
- [22] Dunbar WR, Lior N, Gaggioli R. Combining fuel cells with fuel-fired power plants for improved exergy efficiency. Energy 1991;16:1259–74.
- [23] Ishida M, Kawamura K. Energy and exergy analysis of a chemical process system with distributed parameters based on the energy-direction factor diagram. Ind Eng Chem Process Des Dev 1982;21:690–5.
- [24] Jin H, Ishida M. Graphical exergy analysis of complex cycles. Energy 1993;18:615–25.